D. Fritsch, M. Englich & M. Sester, eds, 'IAPRS', Vol. 32/4, ISPRS Commission IV Symposium on GIS - Between Visions and Applications, Stuttgart, Germany.



# LIKELIHOOD-BASED CLASSIFICATION OF HIGH RESOLUTION IMAGES TO GENERATE THE INITIAL TOPOLOGY AND GEOMETRY OF LAND COVER SEGMENTS:

## "A Hypothesis Generator for Model Based Image Analysis"

**Ali A. Abkar and Nanno J. Mulder**

Division Geoinformatics and Spatial Data Acquisition
International Institute for Aerospace Survey and Earth Sciences (ITC)
P.O. Box 6, 7500 AA Enschede
The Netherlands

Department of Electrical Engineering
University of Twente
P.O. Box 217, 7500 AE Enschede
The Netherlands

## ABSTRACT

This paper's origin is to reach for a way for automatic initiation of shape hypothesis for Model Based Image Analysis (MBIA) in the specific case of agricultural fields. A solution is to start with local (topological) hypotheses. The topological data are integrated from local topology to the level of real 2-dimensional objects. The method requires radiometric model to generate the normalized class membership probabilities (likelihood vectors) and a minimum-size-of-object parameter.

The paper gives a detailed description of the analysis approach for initiating the shape hypothesis for MBIA and besides resolves problems related to classical approaches such as per pixel maximum likelihood classification. An experiment is presented about its application in a case of RGB-CCD image of agricultural fields' model. We obtained an overall accuracy of 97% in comparison with 83% in improved maximum likelihood classification.

**Key words:** Likelihood-based classification, Maximum likelihood classification, Geo-information systems, Remote sensing, Agriculture, Shape hypothesis, Model-based image analysis.

## 1 INTRODUCTION

The application context that is addressed in this paper is to monitor large agricultural areas for land use, crop type and acreage, using remotely sensed data. Therefore, in this context the objects of interest are agricultural fields in the domain of 2-dimensional objects. An agricultural field is defined as a *connected area* with a single crop type. Objects are described by their geometric and radiometric properties. The geometric properties include the position, size, orientation, shape, and topology. The radiometric properties include the reflection properties of the objects and (radiometric) class membership of objects such as agricultural land cover classes (see Figure 1).

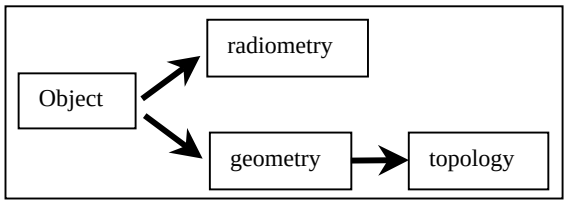


**Figure 1:** The object description

Object topology is defined by a basic data structure Region Adjacency Graph (RAG). RAG is defined as the graph of Nodes and Arcs (N, A), where *N* is the set of nodes and *A* is the set of arcs of the graph [1] and

Node: represents an object with its geometric and radiometric properties,

Arc: represents the (4, 8) adjacency to neighbouring objects.

The above description is valid for static objects only. If the object is dynamic, the description of objects becomes time dependent (temporal property).

Reliable estimates of areas planted with certain crops and of (anticipated) crop production are needed for proper planning, monitoring and improving the development process and policy decisions. Therefore, the classification of agricultural fields in an image of an agricultural area is a key step in this application, which is a good example of the need for integration of Remote Sensing (RS) and geo-information system (GIS).

For detection and classification of agricultural fields using remotely sensed data, the classical classification techniques often fail when only the radiometric properties of the satellite images are used for the classification. In these methods such as Maximum Likelihood (ML) classification, each sample (pixel[1]) is labelled according to its own radiometric properties alone, with no account taken of topological information [2]. Knowledge of neighborhood relationships is a rich source of information that is not exploited in the ML classifiers. For example, in an image of agriculture, adjacent samples are related or correlated, both because imaging sensors acquired significant portions of energy from adjacent samples[2] and because ground cover types generally occur over a region that is large compared with the size of a sample.

In addition, a ML classifier selects the class with the maximum likelihood and it assumes that the other likelihoods for (other) class memberships are zero or negligible. There is often a radiometric overlap between

[1] Pixel: image data sample
[2] This is referred to as the point spread function effect

D. Fritsch, M. Englich & M. Sester, eds, 'IAPRS', Vol. 32/4, ISPRS Commission IV Symposium on GIS - Between Visions and Applications, Stuttgart, Germany.



classes. Some samples in one class may be similar to some (other) samples in another class. Therefore, if we select the maximum likelihood class to which such a sample belongs, it is likely that this may be a wrong decision. Anyway, a choice is made in the case of ML classification, which consequently, is sometimes wrong.

Therefore, in ML classification, the average local error (per pixel) is greater than the average per object error. This approach relies on local error minimisation -- a label is assigned to a sample that is the most probable label based on local evidence.

Mis classification can be partly resolved in several ways. A successful way of reducing mis-classification errors is object based classification using vector and raster mapping, which reduces the error by at least 75%, a figure that is confirmed in many experiments. In fact, accuracies of greater than 95% are achieved in areas of a particularly difficult test case [3][4]. Object based classification integrates gridded or raster images from RS, with agricultural field boundaries or vectors from a GIS, resulting in improved land cover classification. The class label of each object is determined based on the membership of their majority land cover class within the object boundary, assuming that first a per pixel classification is applied. For object based classification the existence of current object boundary data (contained in a GIS) is necessary [3][4].

Here we propose a method where we assume that the object boundaries are not available. In order to overcome the limitations of classical approaches such as per pixel ML classification, we consider in this paper the importance of topological information applied in the set of all likelihood vectors (hypothesis domain).

With the contribution of this research an important step in model based image analysis of remotely sensed data is taken. In the field of remote sensing 3-dimensional CAD models of natural objects are not available. In order to fit geometric models to agricultural fields we develop a method of shape hypothesis generation from local topological models applied in the hypothesis domain. Then, topological data are integrated from local topology to the level of real 2-dimensional GIS objects.

## 2 PROBLEM DESCRIPTION

The importance of this work is defined by the breakthrough of model based image analysis in remote sensing. The prevailing method of image analysis in remote sensing is visual or bottom up. In the previous work by [5][6] that they assumed the field shape hypotheses were generated from an earlier state of the system as recorded in a geo-information system plus rules for changes in crop fields. This is not always possible and the agricultural field boundaries are changing through time because of agricultural practice. Therefore, the problem is that that of automatic initiation of field shape hypothesis generation. Now the scientific question is:

*Is it possible to use image data to generate shape hypotheses constrained by minimal prior knowledge about the shape of agricultural fields?*

In fact, by posing this problem we delay the shape hypothesis generation till we can generate them using the radiometric and topological models applied to the data sets. Therefore, there is a need for intermediate-level processing for shape hypothesis generation, which is the answer to the above question. Once the shape hypotheses are generated we can apply methods of geometric parameter estimation for a typical agricultural field.

A crucial issue in the problem domain, are the constraints provided by the application and requirements of users for development of operational techniques. For an example, Figure 2 illustrates two possible segmentation results of the same wheat field. The segmentation (a), although less coherent, indicates radiometric variation in the southwestern corner which may be due to a change in soil or wind damage. Such information is vital for assessing the possible crop yield from the field. However, in cadastral applications in which the aim is to estimate geometric parameters of single crop units, variations within a field are of no interest and the segmentation in (b) is more appropriate. In this paper the segmentation in Figure 2(b) is of interest.

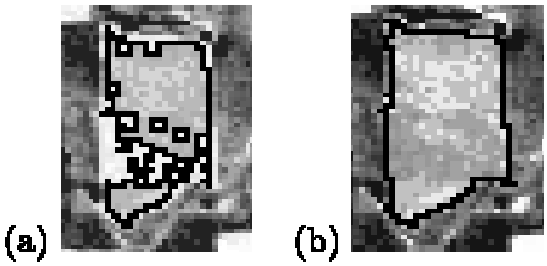


**Figure 2:** Two segmentations of the same crop fields (after [Flack 1995])

## 3 METHOD

As described in our earlier research work [5][7], we generate and calibrate radiometric statistical crop reflection models, which allow us to map M-spectral band data into N-class likelihood vectors, one vector element per class; this is described in the next section. In fitting a shape hypothesis to an actual image field we use the Bayes relationship over combined probability densities of hypotheses. The image data provides the evidence. The hypothesis generator and shape parameters provide the local priors.

Figure 3 illustrates our image analysis method and the relationships between the main components of the analysis process. The essential processing task is the transformation of remotely sensed data into likelihood vectors (evidence). In order to generate likelihood vectors from the remotely sensed imagery relevant training samples are required. Therefore, eight types of land cover classes were selected as training data in the test area: two forest types, one road class, and five crop classes.

A key process within the network is the generation of the initial field shape hypothesis (likelihood-based classification) module. This module generates a sequence of feasible solutions, combining both local topological models and radiometric (information stored as likelihood vectors) constraints to evaluate the relevance of each solution (hypothesis).

Another key process is geometric parameter estimation, the results of which may be directly stored in a GIS as the object parameters.

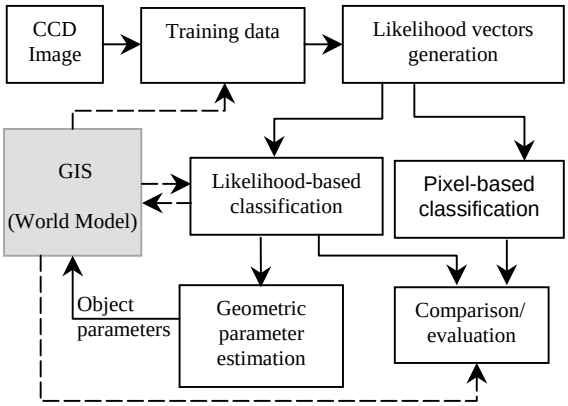


**Figure 3:** Schematic diagram of the image analysis method

An experiment is presented about image analysis application in a case of RGB-CCD image of agricultural fields' model from our Lab. One reason for using the indoor scenes is to concentrate on research rather than on fieldwork; normally our data are from satellite remote sensing sensors. Each processing step is explained in detail below.

The method implemented using Unix-based Khoros 2.2.0 system (http://www.khoral.com).

### 3.1 Generation of likelihood vectors

Radiometric domain is photon counts in several spectral bands at image sample position (i,j) convolved by the sensor point spread function scaled to 0..255; i.e.

Radiometric (Class, Band, {position index (i,j)})

Hereafter abbreviated to **R**, which is the vector of sample values in several spectral bands. We shall denote vectors in boldface type (for instance, **R**, **x**, and **Prob**).

In practice the class probability densities for radiometry are unknown, but for pragmatic reasons we assume that they are normal (Gaussian) with radiometric parameters $\mu$ (class mean) and $\sigma$ (covariance matrix) [8].

We will calculate and store the complete set of likelihood vectors (Prob ($C_1$ | **R**),…, Prob($C_N$| **R**)) i.e. this calculation is a mapping from **R** to the likelihood **Prob**($Class_k$|**R**) under the assumption of equal priors P(Class) in the region of interest.

$$\mathbf{R} \Rightarrow \mathbf{Prob}\ (C_k \mid \mathbf{R})$$

where $C_k$ = ground cover Class k, k=1,2,...,N with N the total number of classes and **R** is the measured radiometry at image sample position (i,j); we also call Prob ($C_k$ | **R**) as *evidence* for class k.

In this section the multispectral images are mapped into the likelihood of class labels per sample. As a result, we generate N channels of probabilities that associates Prob ($Class_1$ | **R**), …, Prob ($C_N$ | **R**)) with samples. Therefore, for each sample, a set of probabilities is available that describes the likelihood that the sample belongs to each of the defined ground cover classes under consideration. Consequently, we will not look only for the class with the maximum likelihood, but also maintain all likelihoods and use them later in the process of image analysis.

The calculation of **Prob**($C_k$ | **R**) for the multivariate case is based on Bayes formula.

The conditional probability for radiometry Prob(**R** | $C_k$) for each class $C_k$, is estimated on the basis of training samples provided by the user. Indeed this is a model for spectral variability of classes in the image. A global estimation of radiometric parameters (class mean and covariance matrix) for specific ground cover classes will influence final classification results negatively. Still, the spectral variability within each class in the image (due to soil differences, moisture content of crop, and crop growing stage, etc.) must be considered. Therefore, radiometric parameters for specific ground cover classes should be constrained in their application to areas and times under which such variables are constant. In many cases this means that radiometric parameters must be defined for each ground cover class locally (spectrally relative homogeneous) in order to minimize radiometric confusion with other classes. In this case the cluster analysis gives an idea about the spectral variability of classes in the image.

Accordingly, to have a better estimation of radiometric parameters of forest class (locally homogenous) in the study area, we have selected two classes for forest namely forest A and B. Latter on in the process of likelihood-based classification the two forests classes were merged to one (global) forest class.

### 3.2 Pixel-based Maximum Likelihood (ML) classification

The local maximum likelihood method (or the maximum a posteriori probability) for image classification aims at assigning a most likely class label $C_k$, from a set of N classes to any sample in the image. It means that we will be looking only for the class with the maximum likelihood and all the other likelihoods are of no interest.

In this experiment, the a priori (global) probabilities were assumed to be the same for all classes.

The ML classification is generally reported to give the highest classification accuracy from remotely sensed data, so we adopted it as our per pixel classifier (see Fig. 7). In this experiment, the threshold for reject fraction-the portion of samples that will remain unclassified due to lowest likelihood of correct classification, was set to 10%. The ML classification is a pixel-based classification (local) in that it labels a pixel on the basis of its radiometric properties alone, with no account taken of geometric or topological information [2][9][10].

### 3.3 Likelihood-Based (LB) classification

Alternatively to the ML classification, the second (third, and N-th) likelihood result were generated, which forms the probability space. In this section, starting at the pixel level in a hypothesis domain (probability space), the local topological hypothesis is initiated. Then topological data are integrated from local topology to the level of real 2-dimensional objects. The process is parallel and iterative. Parallel in the sense that we are dealing with one ground cover class in each step. Iterative in the sense of generating the *Boolean* field shape hypothesis

D. Fritsch, M. Englich & M. Sester, eds, 'IAPRS', Vol. 32/4, ISPRS Commission IV Symposium on GIS - Between Visions and Applications, Stuttgart, Germany.



from local topology to the level of 2-dimensional segments (see Fig. 8). These segments are then used to initiate the field shape hypothesis for geometric parameter estimation. After the geometric parameter estimation the results would be the real 2-dimensional objects of interest with the best-estimated parameters given the minimum cost of error. Generation of 2-dimensional segments is of interest for this paper and the geometric parameter estimation is beyond its scope for this paper.

The detailed analysis of the steps involved are described below:

#### 3.3.1 Thresholding

*Goal is to control the expansion of seed objects.*

Here, the estimated Prob($C_k$ | **R**) for given class $C_k$ was used for which Prob($C_k$ | **R**) < 0.5 was ignored and put to zero, otherwise put to 1. Therefore, in order to control the expansion of a region (explained in the next section), an image (maximum) likelihood threshold was applied to each likelihood image. The spectral overlap between classes is indeed used as a criterion for selection of the threshold. In fact, by selection of the threshold equal to 0.5 (fixed parameter), we selected the local ML class labels for controlling the expansion process only.

#### 3.3.2 Topological operator (structuring element for shrink and expansion)

*Goal is removing enclosed small segments.*

Including the topological information into the classification process can be done by using a simple adjacency surrounding sample (i,j). This can be of any size but, in principle, should be large enough to ensure that all the samples considered to have any spatial correlation with (i,j) are included. For high-resolution imagery of the agricultural environment this is practical and simple 3×3 adjacencies such as shown in Figure 4 can be adopted.

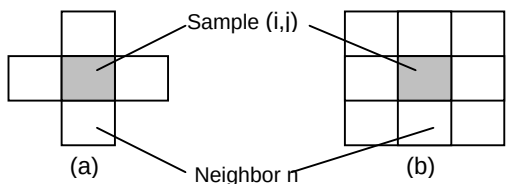


**Figure 4:** Definition of a simple adjacency about sample (i,j)
(a) 4-connected
(b) 8-connected

#### 3.3.3 Local min operator (shrinking with size constraint)

*Goal is seed generation.*

The object-size-hypothesis and shape of structuring element are used as parameters.

Now assume that a neighborhood function can be defined which allows the samples in the prescribed neighborhood to influence the possible likelihood of sample (i,j). For example, if a likelihood component is examined in 3 × 3 windows as described above, a label at the center of the window might be changed to the smallest likelihood represented in the window. Clearly this must be done carefully, with the user having some control over the minimum size region of a given cover type that is acceptable. Such a modification is made to the set of likelihoods for all samples by moving over the image from its top left hand to bottom right hand corners. This process is applied as many times as necessary to ensure that the seed objects have been generated.

In this experiment, the local min operator was used as a variable parameter with two possibilities 6 or 7 (the number of iterations) to generate the seed objects. Seed object generation is done for each class separately using the likelihood component of that class. Estimation of the right parameter value for the local min is very important especially in case we have overlap in radiometry, because we may come up with false objects or destroy the topology of the existing objects. These types of errors sometimes cannot be corrected in the later process.

As a result, local min operation will remove the mixed pixels/enclosed small segments (a major source of mis-classification error), which will enable a purer selection of pixels (geometry knowledge) and hence radiometric properties to be used for determining the shape and land cover type for the object.

#### 3.3.4 N-conditional dilation on Boolean

*Controlled expand operation by maximum likelihood threshold in the hypothesis domain.*

In this phase we grow the seed objects generated in the previous phase. N-conditional dilation will do N successive conditional expansion of the seed object by defined the 3 × 3 structuring element, using the thresholded likelihood image as a conditional image for expansion. This means that a region cannot grow further than in the thresholded likelihood image. The number of successive expansions can be fixed if we set N to a high number e.g. 100. It does not depend on any other parameters such as the number of iterations for local min. The reason for this is the control of expansion by the maximum likelihood threshold in the hypothesis domain. After a certain number of successive expansion and removing/filling the enclosed small segments, this parameter is no longer sensitive and will change nothing.

### 3.4 Geometric (shape) parameter estimation

This stage is beyond the scope of this paper and would be the next challenge. We generate a hypothesis boundary without giving a parametric description at this stage.

## 4 EXPERIMENTAL DATA AND RESULTS

| | |
|---|---|
| Image format: | one color CCD video camera image, i.e. three bands R/G/B (see Fig. 5); |
| Image size: | 576 × 768 (rows/cols); |
| Ground truth: | different GIS-layers: roads, farm houses, forests and five different crop fields for evaluation of the results (see Fig. 6); |
| Selected classes: | two classes of forest, five classes of crops, and one class of road, making in total eight radiometric classes; |
| Aim: | classification of forests and crop classes. |

The RGB image has been digitized for use as a ground truth for generation of radiometric parameters

(class signatures) and quality assessment (see Fig. 6). The radiometric parameters in terms of means and covariance matrices were estimated for all the eight classes from the training samples. These parameters were used to generate the likelihood vectors **Prob**($C_k$|**R**) as discussed in the previous sections. In the process of likelihood-based classification the two forests classes were merged to one (global) forest class (see Fig.6 and Fig.7).

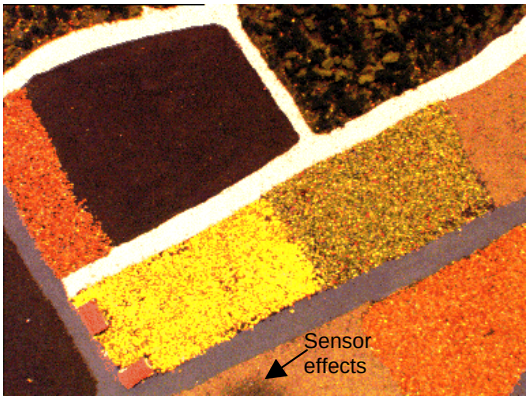


**Figure 5:** Shows RGB-CCD image (image size: 576 rows × 768 cols)


**Figure 6:** Land use map of the test area including one class of forest, five classes of crops, two classes of roads, and one class of farm houses (obtained by hand segmentation).

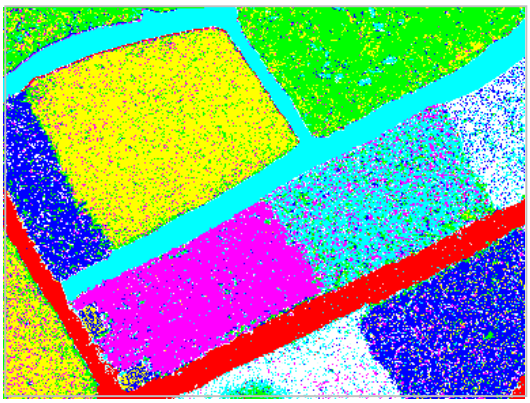

**Figure 7:** Shows the maximum likelihood classification per sample (7 classes)

The image was also classified on per pixel basis by the ML classifier, for comparison with the result of the likelihood-based classification applied in the hypothesis domain described in the last section.

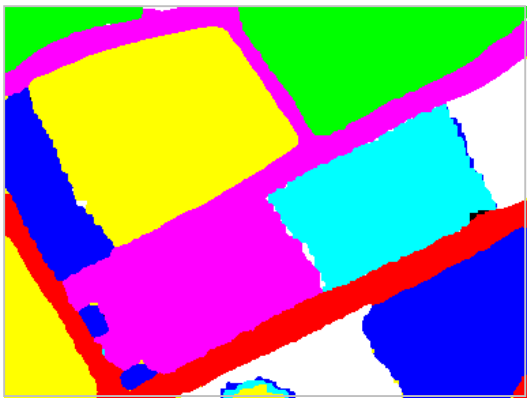

**Figure 8:** Shows the final result of likelihood-based classification. This Figure shows the result of local hypotheses testing resulting in a segmented image. Small segments have been removed and shape hypotheses initiated.

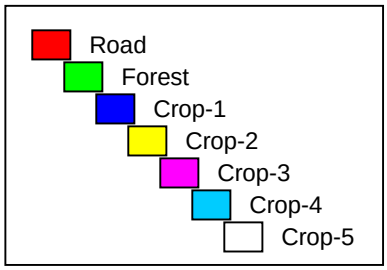


Legend for Fig. 7 and Fig.8

## 5 EVALUATION

There are a number of observations that can be made about these results. The most obvious of these are about uncertainty in final classification. Uncertainty in the final classification is caused by the following uncertainties [11][12][13][14][15]:

(a) Source image e.g. due to image acquisition, sensor, platform, atmospheric conditions, etc.
(b) Spectral variability within each class in the image due to soil differences, moisture content of crop, and crop growing stage (definition of crop radiometry), etc.
(c) Spatial variability within each class due to complex natural phenomena such as topology, geology, and relief (definition of crop fields geometry/shapes)
(d) Image classification methodology due to training samples, use of classification algorithms, non-normal class distribution.

For an example about uncertainties in the source images (a) see Figure 5 (bottom center of the image).

Classification uncertainties that arise due to spectral variability within each class in the image and the sampling procedure (b and d), for example, include:

D. Fritsch, M. Englich & M. Sester, eds, 'IAPRS', Vol. 32/4, ISPRS Commission IV Symposium on GIS - Between Visions and Applications, Stuttgart, Germany.



❑ *Local estimation of radiometric parameters:*
Radiometric parameters for specific ground cover classes should be constrained in their application to areas and times under which such variables are constant. In many cases this means that radiometric parameters must be defined for each ground cover class locally (spectrally relative homogeneous) in order to minimize radiometric confusion with other classes.

❑ *The geometric accuracy of the source data:*
Especially in spatially complex situations it may be difficult to locate the training samples on an image.
❑ *The spatial resolution of the image:*
If the sample size of the image is larger than the area in which crop types occur, the sample will not contain a homogeneous area.

Classification uncertainties that arise due to the algorithm (d) include:
❑ *Gaussian (normal) class distribution*
Assumption of normality for class probability distribution of each ground cover class is the mathematical simplification of the real world; this is not a correct assumption.

### 5.1 Quantification of uncertainty

In order to assess the accuracy of the classified results, the confusion (error) matrix was created. In this paper the overall accuracy (the fraction of all ground truth samples that are classified correctly) from the confusion matrix is used to compare the results of likelihood-based (LB) classification and Maximum Likelihood (ML) classification (See Table 1). The two approaches (LB and ML) are applied to a color CCD image and the results are evaluated by comparison with *ground truth* obtained by hand segmentation.

For comparing also our result with the improved ML classification result, a 3×3 Zero-majority filter is applied to the result of ML classification to classify some unclassified samples. Afterward, a 3×3 Majority filter is applied to the Zero-majority result to smooth the classified result (See Table 1).

**Table 1:** Accuracy assessment of the developed method as compared with the ML results

| Methods | Overall accuracy |
|---|---|
| LB classification | 97.53 |
| ML classification | 66.56 |
| Filtering results | 83.37 |

Although in this specific case filtering improved the overall accuracy, in general, filtering may be considered as area specific *cosmetics*. It may be applied to an area if there is radiometric confusion, but, in general, it may shift the original object boundary.

A further comparison of our result with the ML result was done using the object boundaries of the ground truth map obtained by hand segmentation for the evaluation (see Fig. 6 and Fig. 9). For this comparison first, a raster to vector conversion is done.

Figure 10 shows the extracted segments using the final result of ML classification compared with the object boundaries of the ground truth map. This Figure shows the mixed (boundary) pixels and mixed pixels within fields. Due to these mixed classified pixels, ML classification often yields uncertain or erroneous results.
Figure 11 shows the extracted segments using the final result of likelihood-based classification. This Figure shows the result of local hypotheses testing resulting in a segmented image. Small segments have been removed and shape hypotheses initiated.

**Figure 9:** The object boundaries of the ground truth map obtained by hand segmentation (the ground truth map is shown in Fig. 6)

**Figure 10:** shows the object boundaries of the ground truth map (blue) superimposed to the improved maximum likelihood results (red)

**Figure 11:** shows the object boundaries of the ground truth map (blue) superimposed to the likelihood-based classification results (red)

## 6 CONCLUSION

Based on the proposed method for image classification and automatic shape hypotheses generation, several conclusions may be derived as follow:

- it is simple, quick, and easily implemented,
- it is efficient because it deals only with likelihood vectors (classes) and not with spectral values in the image,
- it is relatively simple to include GIS data such as infrastructure and topological information as constraints on hypothesis generation and parameter estimation,
- an overall accuracy of 97% was obtained in comparison with 83% in improved maximum likelihood classification.
- the algorithm can create irregularly shaped segments, and
- development of a hypothesis boundary generator for model based image analysis.

### 6.1 Future work

As a result of this study the followings are recommended for further attention and studies:

- Applying the local topology “local max” controlled by threshold in the hypothesis domain and re-normalization of the likelihoods.
- Incorporating region adjacency graph (explicitly) into the process of image analysis. From topology graph we may derive how to remove the enclosed small segments.
- Parametric edge/shape hypothesis generation and testing
- It is recommended to define ground cover classes at the highest possible hierarchical and detailed level related to the aim of the research (local estimation of radiometric parameters for each ground cover class).
- multisource data analysis in the hypothesis domain instead of image domain (image fusion).

### Acknowledgments

The authors would like to thanks Dr. M.J. Korsten for his help during the implementation of this work using Khoros system and Prof. P.P.L. Regtien, Ir. Z. Houkes, and Dr. M.A. Sharifi for their comments on the manuscript.

### REFERENCES

[1] Nichol, D. G. (1990). Region adjacency analysis of remotely-sensed imagery. International Journal of Remote Sensing, 11(11), 2089-2101.

[2] Richards, J. A. (1993). Remote Sensing Digital Image Analysis: An Introduction. 2nd ed., Springer-Verlag, Heidelberg, Germany.

[3] Janssen L.F., M.N. Jaarsma, and E.T.M. van der Linden (1990). Integrating Topographic Data with Remote sensing for Land-cover Classification. Photogrammetric Engineering & Remote Sensing 56(4): 1503-1506.

[4] Abkar, A.A. (1994). Knowledge-Based Classification Method for Crop Inventory Using High Resolution Satellite Data. MSC Thesis, ITC, Enschede, The Netherlands.

[5] Mulder, N.J. (1994). A theory of knowledge based image analysis with applications to SAR data of agriculture. Proceeding of European Optical Society and International Society of Optical Engineering Symposium, 26-30 Sept. 1994, Rome, Italy.

[6] Mulder, N.J. and Fang Luo (1994). Knowledge based image analysis of agricultural fields in remotely sensed images. Pattern Recognition in practice, Vlieland.

[7] Abkar, A.A. and N.J. Mulder (1996). A Comparison between Top-Down and Bottom-Up Image Analysis in Terms of the Complexity of Searching a Problem Space. IAPR Workshop on Machine Vision Applications (November 12-14, 1996), Keio University, Tokyo, Japan, 1996.

[8] Ripley, B.D. (1996). Pattern Recognition and Neural Networks. Cambridge University Press, ISBN 0 521 46086 7. P.21 & p.329.

[9] Jensen, John R. (1996). Introductory Digital Image Processing. 2nd ed. Chapter 8, Thematic Information Extraction: Image Classification. Upper Saddle River, NJ: Prentice-Hall. pp. 229-231.

[10] Lillesand, Thomas M. and Kiefer, Ralph W. (1994). Remote Sensing and Image Interpretation. 3rd ed. Gaussian Maximum Likelihood Classifier in Chapter 7, Digital Image Processing. New York: John Wiley and Sons. pp. 594-596.

[11] Campbell, J.B. (1987). Accuracy assessment. In: J.B. Campbell. Introduction to Remote Sensing. The Guilford Press, New York, London.

[12] Congalton, R.G. (1988). A comparison of sampling schemes used in generation error matrices for assessing the accuracy of maps generated from remotely sensed data. Photogrammetric Engineering & Remote Sensing 54(5): 593-600.

[13] Lunetta, R.S., R.C. Congalton, L.K. Fenstermaker, J.R. Jensen, K.C. McGwire & L.R. Tinney (1991). Remote sensing and geographic information system data integration: error sources and research issues. Photogrammetric Engineering & Remote Sensing 57(6): 677-687.

[14] Palacio-Prieto, J.L. & L. Luna-Gonzalez (1996). Improving spectral results in a GIS-context. Int. J. Remote sensing 17(11), 2201-2209.

[15] Shi, W.Z. & M. Ehlers (1996). Determining uncertainties and their propagation in dynamic change detection based on classified remotely sensed images. Int. J. Remote Sensing 17(14).

[16] Flack J. (1995). Interpretation of remotely sensed data using guided techniques. School of Computer Science, Curtin University of Technology, Western Australia. http://www.per.dem.csiro.au/staff/FlackJulien/thesis/node2.html